PAP-452

FLOW PASSAGE DESIGN FOR BULB TURBINE INTAKES

C. A. Pugh, Hydraulic Engineer
Hydraulics Branch, Division of Research
Engineering and Research Center
Bureau of Reclamation
United States Department of the Interior
Denver, Colorado

ABSTRACT

Intakes for bulb or rim generator turbines are very large in relation to the runner diameter. Because the velocity is low in the intake area, the losses are also low. This report describes research on the effect of simplifying intake design on energy losses and flow distribution. Using straight surfaces in place of curved bellmouth entrances and shortening the length of the intake could significantly reduce construction costs. In addition, reducing the intake size would reduce the size of the trashracks, gates, and associated operating equipment.

NOMENCLATURE

A_r = flow area at the runner = $0.6535(D1)^2$
C_p = pressure drop coefficient
D = reference length
d/D = relative depth in intake
D1 = runner diameter
E = Euler number
H = gross head
g = acceleration of gravity
Q = flow rate or discharge
R = Reynolds number
V = velocity
V_I = average intake velocity in the axial direction
V_r = average runner velocity in the axial direction = Q/A_r
$\overline{V}$ = average velocity
Δh = relative loss
Δp = pressure drop
θ = wicket gate angle
ν = kinematic viscosity
ρ = density
γ = specific force = ρg
γ_a = specific force of air

INTRODUCTION

The main obstacle in the development of small hydropower has been economics. In most cases, the cost per installed kW (kilowatt) is still higher than for fossil fuel plants. For low-head hydroelectric installations, head less than 20 m, the major cost is the initial investment in the civil works structure and the fluid machinery. If the cost of the structure can be reduced without introducing additional losses, more small hydroelectric installations would be feasible.

Intakes for bulb or rim generator turbines are very large in relation to the runner diameter. Because the velocity is small in the intake section, the losses are also small. It was concluded in an earlier literature review (1) that savings could be achieved by replacing curved surfaces with straight surfaces and shortening the length of the intake. Reducing the intake size would also result in additional savings in trashracks, entrance gates, and associated operating equipment.

Another small hydropower reference (2) stated that "Irregularities of flow as well as flow separations in the intake section have an unfavorable effect on the turbine's hydraulic behavior, and an optimum design for the intake portion is therefore essential for smooth undisturbed turbine performance." However, the data presented herein demonstrate that simplifications in the intake section do not adversely affect the flow field leading to the guide vanes and runners.

SCOPE OF STUDY

A model of a typical bulb turbine was built as a basis for comparison with other intakes (fig 1). The model dimensions basically correspond to standard flow passage dimensions used by a major manufacturer. The intake section of the model was removable.

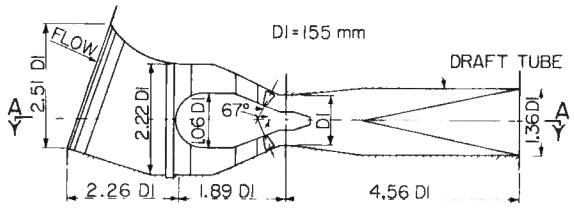

SECTION THROUGH BULB TURBINE MODEL

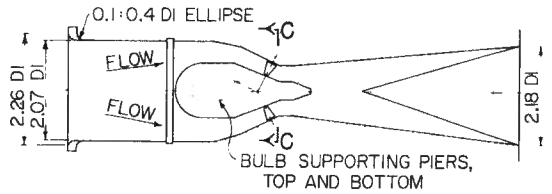

SECTION A-A

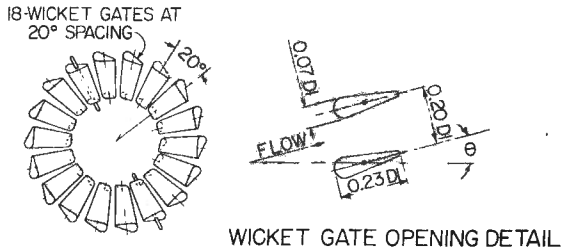

WICKET GATE OPENING DETAIL

SECTION C-C

Fig. 1 Bulb turbine model.

After testing the original intake, three other intakes of various shapes and sizes were tested and the results compared (fig 2). Dimensions are given in terms of runner diameter (D1).

Extensive testing was done on the original intake to determine the effect of a bulkhead slot, a pier in the intake, a draft tube, and various approach channel configurations.

MODEL DESIGN AND SIMILARITY

An air model was used to study flow in the intake section. There are several reasons for using an air model instead of a water model, including (a) flexible, easy model construction; (b) little problem of leakage; and (c) quick model measurements and changes. The disadvantages are (a) small levels of pressure differences requiring delicate measuring apparatus and (b) inability to simulate a free surface. Air models can be used to study hydraulic problems in which the flow is governed by inertia and viscosity effects. (3) Conditions of flow at an entry and flow through pressurized conduits fall within this category. The criterion of similarity for this type of flow and for transferring results to prototype conditions is well known to be the Reynolds model law (equation 1).

$$\text{Reynolds number} = R = \frac{VD}{\nu} \qquad (1)$$

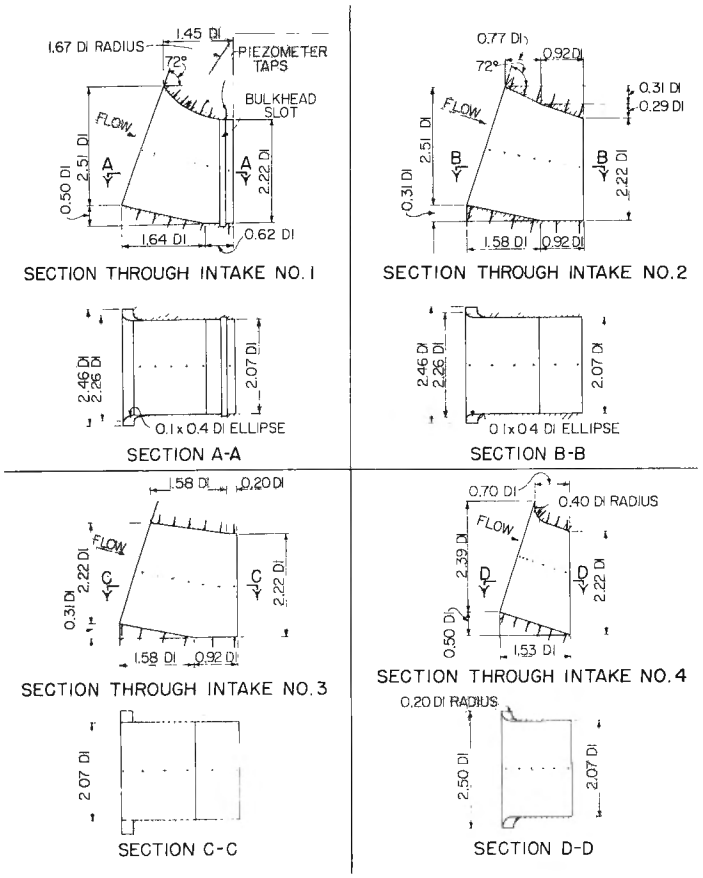

Fig. 2 The four intakes tested.

Most prototype hydraulic structures have Reynolds numbers of the order of magnitude of 10^6 to 10^8. The achievement of these Reynolds numbers under laboratory conditions would require blowers with enormous capacity. It is possible, however, to attain approximate similarity at Reynolds numbers of about 10^4 to 10^5. At these Reynolds numbers viscosity has little effect. It is also necessary to build the model large enough to avoid undesirable compressibility effects. In general, the air velocity should not exceed 50 m/s. The model was designed to keep the Reynolds number as high as possible while keeping the air velocity less than 50 m/s.

The Euler number is a dimensionless ratio which relates inertia forces to pressure forces (equation 2).

$$\text{Euler number} = E = \frac{\rho V^2}{\Delta p} \qquad (2)$$

In incompressible fluids and in the absence of other forces (such as viscosity and gravity), the Euler number is exclusively a function of the geometry of the flow boundaries. (3) At Reynolds numbers high enough to attain similarity, the Euler number is constant. Therefore, the Euler number will be the same for any prototype size as it is in the model if the geometry is similar. For this reason, the Euler number is also referred to as the geometrical flow number.

The first set of tests was conducted to determine the minimum discharge to obtain similarity. Tests were run at different discharges for the same model configuration. At Reynolds numbers greater than 10^5 the Euler number is approximately constant (fig 3). Therefore, all of the tests were conducted at Reynolds numbers greater than 10^5. The Euler number is then used to scale results from the model to prototype conditions.

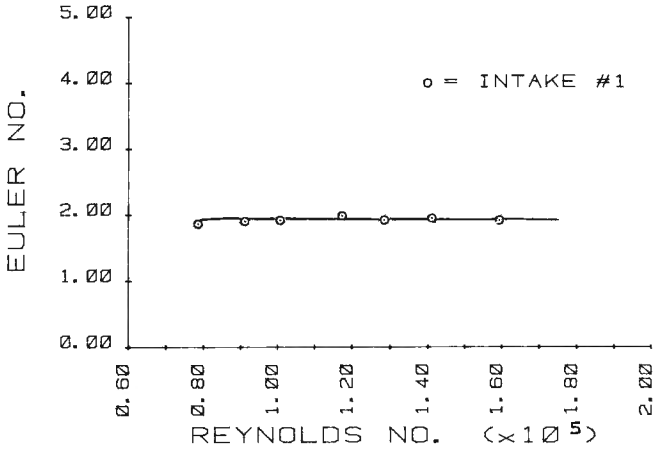

Fig. 3 Euler number vs Reynolds number.

THE MODEL

Figure 4 is a schematic diagram of the testing apparatus. Air is supplied from a blower through a supply line and orifice plate into a stilling chamber (plenum). The pressure in the plenum forces the air through the model.

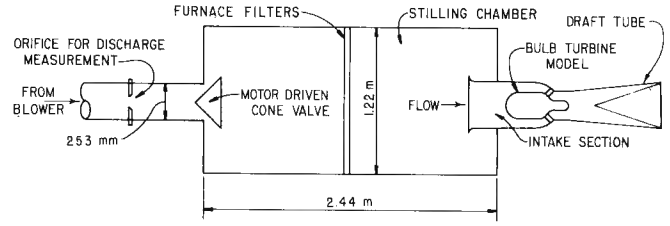

Fig. 4 Schematic diagram of apparatus.

The intake sections were made of sheet metal. Piezometer taps were included along the top, bottom, and sides of each intake to measure the pressure drop along the surfaces (fig 2). A pressure tap was also included in the plenum to measure the total pressure required to produce a given flow through the model.

The main part of the model and the draft tube were made from transparent Plexiglas. The wicket gates and bulb were formed from wood and the bulb supporting piers were made of high density polyurethane. Figure 5 is an overall photograph of the testing apparatus and figure 6

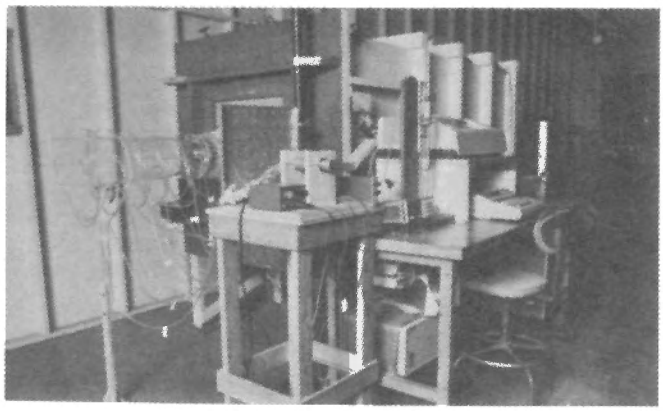

Fig. 5 Overall photograph of testing apparatus.

shows a closeup photograph of intake 1. The wicket gates were operated simultaneously with a control ring. Figure 1 contains a definition sketch for the wicket gate opening angle (θ). θ was adjustable from 0 to 60 deg, with 0 deg being full open. Runner blades were not included in the model because the focus of the study was the effect of changes in the intake flow passage geometry. The changes in Euler numbers due to changes in flow passage geometry are not affected by the runner blades.

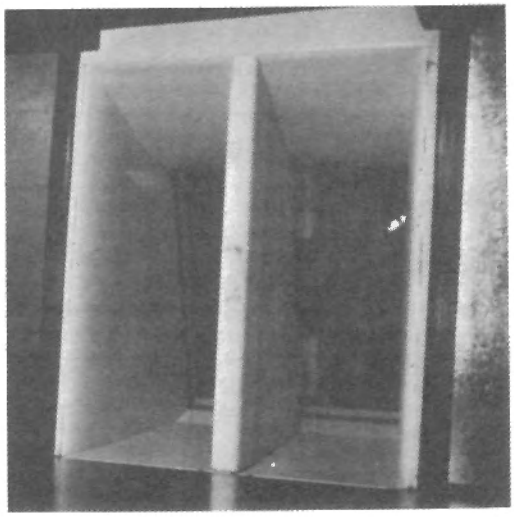

Fig. 6 Photograph of intake 1 with center pier, approach channel with bottom, no sides (looking downstream from inside plenum).

TEST PROCEDURES AND INSTRUMENTATION

Data collected during the tests included (a) total discharge through the model; (b) velocity profiles just upstream from the bulb (at the bulkhead slot in fig 1); (c) pressures along the top, bottom, and sides of the intake being tested; and (d) plenum and atmospheric pressures.

Discharge Measurement

The rate of flow or discharge was measured with a concentric, thin plate orifice located in the supply line (fig 4). Flange taps just upstream and downstream from the orifice plate were used to obtain the pressure differential across the plate. Working equations for computing actual rates of flow through an orifice plate are found in "Fluid Meters - Their Theory and Application." (4)

Velocity Measurement

Velocity measurements were made for each intake at various wicket gate openings at the bulkhead slot location just upstream from the bulb (fig 1).

A hot wire, constant temperature anemometer was used to measure air velocity. Velocity was measured at 117 points in a 9 by 13 grid using a telescoping probe attached to the self-contained instrument. The readings were recorded manually. The hot wire anemometer readings were checked by measuring known velocities through an orifice in the side of the stilling chamber.

Pressure Measurement

The pressure differences in an air model are small. Therefore, sensitive and accurate instruments are needed to collect acceptable data.

Pressure taps from the orifice plate, in the intake, and in the plenum were connected to a single scanning-type pressure sampling valve for measuring multiple pressures. Using this system one pressure transducer was used to measure all the pressures. A manually operated step drive was used to connect each pressure line sequentially to the center port of the valve. The center port was connected to a $\pm$6.895-kPa differential pressure transducer. The transducer has a total error of 0.06 percent (combined linearity and hysteresis).

The transducer excitation was 12 V d c, the output was amplified by 1,000 times with a high gain data amplifier. The amplified output was in the range of -5 to +8 volts. The opposing side of the differential transducer was open to atmospheric pressure. The output voltages were read with a high speed (DVM) digital voltmeter. The data were collected and stored using a data acquisition system. A microprocessor (fig 5) was programmed to read average and fluctuating voltages from the DVM. The voltages were converted to pressures, and when the test was complete, the data were transferred from memory to cassette tape for later printing, plotting, and analysis. Atmospheric pressure was recorded before and after each test to ensure that the reference did not vary substantially during the test.

RESULTS

Velocities

Velocity distributions were plotted for each intake (at θ = 30 deg) (fig 7). The average velocity ($\overline{V}$) is different for each intake; however, the flow distribution is not affected by the actual values of velocity if the Euler number is constant (see the previous section on similarity).

It is obvious from comparing the velocity contours that the intake shape has a significant effect on velocity distribution (see fig 2 for intake shapes). The

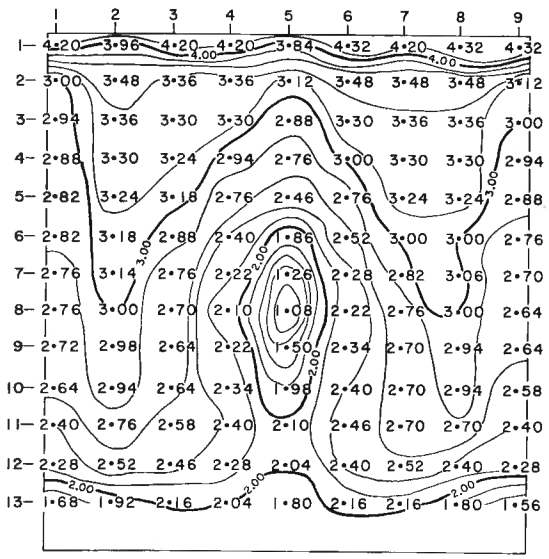

INTAKE NO. 1 – $\bar{V}$ = 2.837 m/s

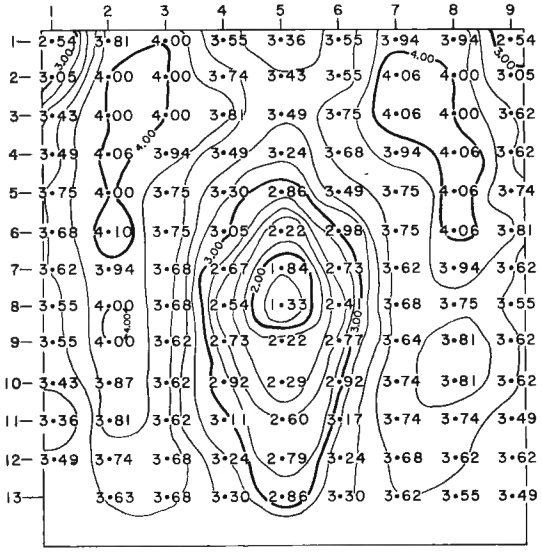

INTAKE NO. 2 – $\bar{V}$ = 3.363 m/s

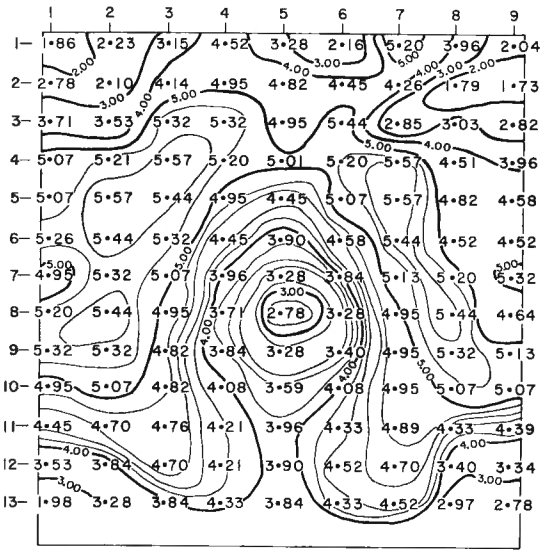

INTAKE NO. 3 – $\bar{V}$ = 4.288 m/s

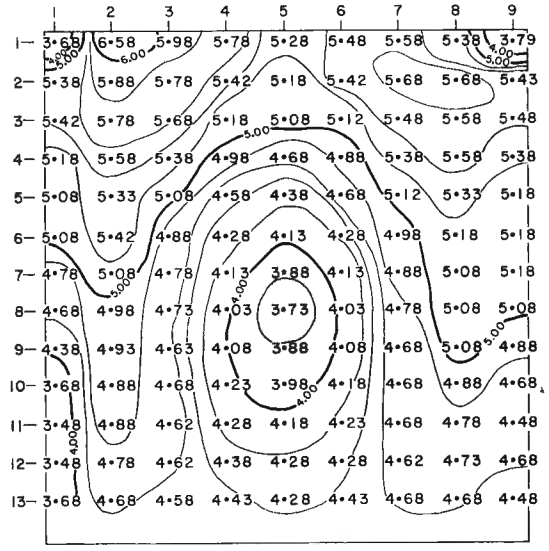

INTAKE NO. 4 – $\bar{V}$ = 4.552 m/s

Fig 7 Velocity distributions in the intakes ($\theta = 30^{0}$).

velocity distributions for all four intakes show the flow stagnating in front of the bulb and flowing around it to the sides.

In intake 1 the velocities are high near the top (due to the smooth bellmouth-type top curve) and low near the bottom, with a steep transition from top to bottom.

In intake 2 the velocities are fairly uniform throughout; the local velocities do not vary greatly from the average velocity.

Intake 3 does not have intake curves; the corners are square. The effect of the square corners is apparent in the velocity distributions. Velocities are high through the center portion of the profile and very low at the edges and corners.

The flow distribution in intake 4 is fairly uniform. The pattern does not indicate high velocities in the center (as in intake 3), or a steep gradient from top to bottom (as in intake 1).

The velocity profiles from top to bottom along data column 3 in figure 7 are plotted on figure 8. This graph illustrates the differences in flow distribution between the four intakes in the zone where the majority of the flow passes around the bulb. Intakes 2 and 4 have the most uniform profiles.

It should be noted that average velocity head ($\bar{V}^2/2g$) in the intake section is usually only about 1 percent of the total prototype head. Therefore, flow irregularities in the intake section should have a relatively minor effect on losses in the intake section. However, a nonuniform flow distribution at the wicket gates and runners could have an effect on losses and smooth turbine operation.

Table 1 Pressure drop through model

Wicket gate angle (degrees)	Model with draft tube/approach channel bottom - no sides: Intake 1 E	Intake 1 Run No.	Intake 2 E	Intake 2 Run No.	Intake 3 E	Intake 3 Run No.	Intake 4 E	Intake 4 Run No.	Intake 1 with pier E	Intake 1 with pier Run No.	Model with draft tube, Intake 3, No approach channel E	No approach channel Run No.	Approach with both sides E	Approach with both sides Run No.
0	4.321	149	4.178	166	4.195	186	4.173	197	4.121	140	4.137	175	4.227	180
15	3.535	150	3.425	167	3.435	187	3.559	198	3.549	141	3.709	176	3.389	181
20	2.360	162	2.349	171	-	-	-	-	2.407	145	-	-	-	-
25	1.728	163	1.754	172	-	-	-	-	1.748	146	-	-	-	-
30	1.297	151	1.322	168	1.290	188	1.340	199	1.258	142	1.384	177	1.278	182
35	0.925	164	0.967	173	-	-	-	-	0.941	147	-	-	-	-
40	0.683	165	0.709	174	-	-	-	-	0.674	148	-	-	-	-
45	0.499	152	0.500	169	0.506	189	0.491	200	0.499	143	0.519	178	0.551	183
60	0.153	153	0.168	170	-	-	0.158	201	0.161	144	0.163	179	0.164	184-185

Wicket gate angle (degrees)	Intake 1 without draft tube, Approach channel: With both sides E	With both sides Run No.	With both sides (lowered) E	With both sides (lowered) Run No.	With one side E	With one side Run No.	With bottom (no sides) E	With bottom (no sides) Run No.	With bulkhead slot with both sides E	With bulkhead slot with both sides Run No.	Intake 4 with draft tube, No approach channel E	No approach channel Run No.
0	1.810	120	1.813	129	1.814	134	1.821	137	1.808	101-104	3.915	192
15	1.648	121	1.650	130	1.644	135	1.650	138	1.662	105-107	3.509	193
20	1.465	125	-	-	-	-	-	-	-	-	-	-
25	1.210	126	-	-	-	-	-	-	-	-	-	-
30	0.984	122	0.985	131	0.997	136	0.975	139	1.000	108-110	1.015	194
35	0.768	127	-	-	-	-	-	-	-	-	-	-
40	0.567	128	-	-	-	-	-	-	-	-	-	-
45	0.411	123	0.413	132	-	-	-	-	0.399	117-119	0.380	195
60	0.143	124	0.140	133	-	-	-	-	0.145	115-116	0.178	196

Pressures

An indication of the accuracy of the Euler numbers is needed in order to determine if the differences are due to geometry changes or data scatter. Therefore, several runs were made for the same geometry at different discharges in runs 101 through 116. The Euler numbers varied by ±0.015; therefore, changes greater than 0.015 are due to geometry effects rather than data scatter.

Pressure drop through the entire model as well as pressures along the flow surfaces in the intake section were measured for each test run. Table 1 lists the Euler numbers for the different configurations tested. These data can be used to assess the effect of changes in geometry on pressure drop (losses) through the model. The table also defines the model configuration for each run number. The reference velocity used in the Euler number in table 1 was the average axial velocity at the runner (V_r).

The data in table 1 can be used to compare relative losses between different geometries. For example, the relative losses in the four intakes can be compared.

From equation (2) $\Delta p = \frac{\rho V^2}{E}$ and in terms of head,

$$\frac{\Delta p}{\gamma} = \frac{V^2}{gE} \qquad (3)$$

Taking the difference of equation (3) for two configurations, the relative losses between two configurations (Δh) are

$$\Delta h = \frac{\Delta p_2}{\gamma} - \frac{\Delta p_1}{\gamma} = \frac{V^2}{g}\left(\frac{1}{E_2} - \frac{1}{E_1}\right) \qquad (4)$$

for equivalent discharges.

Equation 4 shows that the relative losses are proportional to velocity head. Therefore, actual losses will be more for higher discharges if the Euler number is the same.

Example calculation of relative losses. For a hypothetical prototype installation, the following values are given:

The runner diameter = D1 = 3.51 m
The area at the runner = A_r = 8.03 m^2
The prototype head = H = 13.52 m
The discharge relationship
at θ = 0 deg, Q = 127 m^3/s
at θ = 15 deg, Q = 85 m^3/s
at θ = 30 deg, Q = 43 m^3/s

Since $V_r = Q/A_r$, $V_r(\theta = 0\ deg) = 15.82$ m/s,
$V_r(\theta = 15\ deg) = 10.58$ m/s, and
$V_r(\theta = 30\ deg) = 5.36$ m/s.

The Euler numbers in table 1 can be used to compute the relative head losses - using equation 4. Table 2 gives relative head losses for this example using intake 1 as a reference.

Table 2 Comparison of intake losses

	θ = 0° Δh(m)	θ = 0° Δh/H(%)	θ = 15° Δh(m)	θ = 15° Δh/H(%)	θ = 30° Δh(m)	θ = 30° Δh/H(%)
Intake 2	0.202	1.5	0.104	0.8	-0.043	-0.3
Intake 3	0.178	1.3	0.094	0.7	0.012	0.1
Intake 4	0.210	1.6	-0.022	-0.2	-0.073	-0.5

Table 2 shows that (for this example) intake 1 has about 1.5 percent less loss than the other intakes when the wicket gates are full open (θ = 0 deg). However, when the gates are partially closed (θ = 15 and 30 deg), intake 4 has less loss than intake 1. Intake 2 has less loss at θ = 30 deg. This is consistent with the velocity comparisons (figs 7 and 8) showing that intakes 2 and 4 have a more uniform velocity distribution than intake 1.

Pressure drop coefficients. Another form of the Euler number is the pressure drop coefficient (C_p). The pressure drop coefficient is the ratio of drop in pressure head to a reference velocity head (equation 5).

$$\text{Pressure drop coefficient} = C_p = \frac{(\Delta p/\gamma)}{(V^2/2g)} \qquad (5)$$

It can be shown by combining equations 2 and 5 that $C_p = 2/E$ and equation 4 becomes

$$\Delta h = V^2/2g(C_{p2} - C_{p1}) \qquad (6)$$

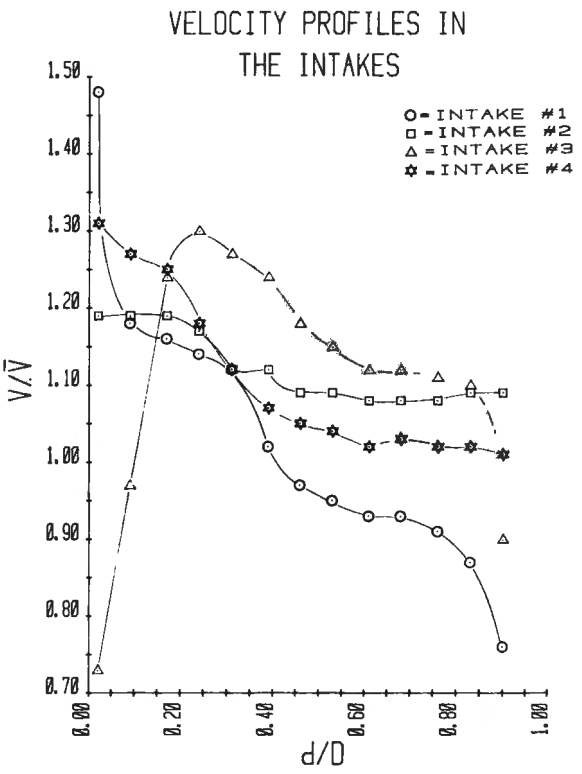

Fig. 8 Velocity profiles along data column 3 on figure 7.

Plotting C_p allows observation of losses in terms of a reference velocity head. Figure 9 is a comparison of pressure drop coefficients for the four intakes. About 48 percent of the velocity head at the runner (C_p = 0.48) is required to produce the flow through the model (for θ = 0 deg). The plot illustrates the relative importance of intake losses to the overall losses. Intake 3, with no entrance curves, has the highest losses. However, even with no attempt to streamline the entrance, the losses in intake 3 are not significantly higher than in the other intakes. Intakes 2 and 4, with simplified and shortened intakes, show lower losses for partial gate openings than the traditional bellmouth-type design (intake 1) and have a more uniform velocity distribution.

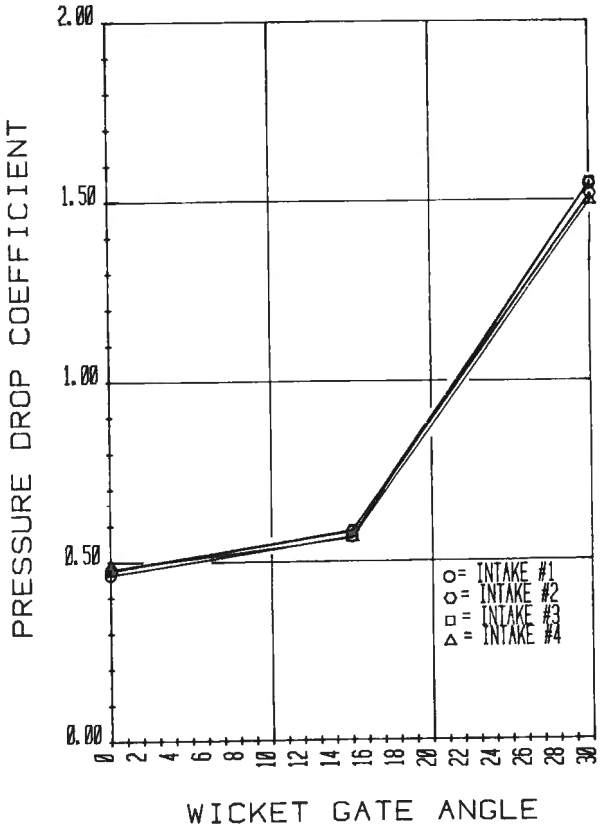

Fig. 9 Pressure drop (C_p) through the model - comparison of four intakes. Uncertainty of C_p is $\pm$0.015.

Additional testing. Extensive testing was done on intake 1 to determine the effect of other geometric features including:

1. A bulkhead slot
2. A center pier in the intake
3. The approach channel configuration
4. A draft tube

The Euler numbers in table 1 illustrate that the bulkhead slot has essentially no effect on losses, and the center pier and approach channel have little effect on the losses in intake 1. However, the approach channel did have a significant effect in one case. The Euler numbers for intake 4 without an approach channel are lower than intake 4 with an approach channel bottom, except for θ = 60 deg (see table 1, runs No. 192-196 vs 197-201). Tests on intake 1 did not show a significant effect due to the approach channel (runs No. 101-139). This difference can be explained by referring to figure 8. The relative velocity at the bottom of intake 1 is very low compared to intake 4. Therefore, the approach channel (which guides the flow into the bottom of the intake preventing flow separation along the bottom) would be more important in intake 4 than in intake 1.

Although the draft tube does not affect intake losses, tests were run with and without a draft tube to determine the relative importance of the draft tube to the overall losses. The draft tube recovered about 60 percent of the runner velocity head. The losses through the model with the draft tube were less than one-half of the losses without the draft tube (at θ = 0 deg).

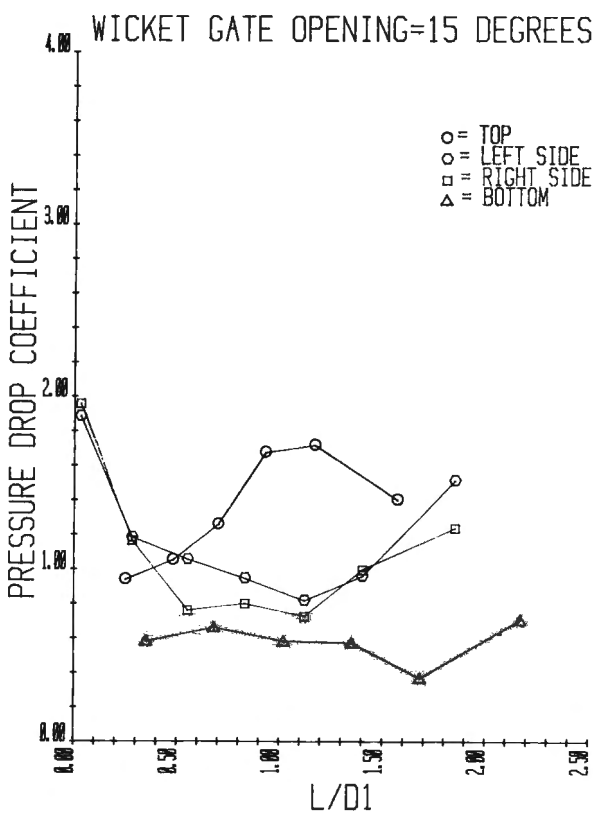

Fig. 10 Pressure drop (C_p) along intake surfaces - intake 1. The uncertainty of the intake pressure drop coefficient is ±0.10.

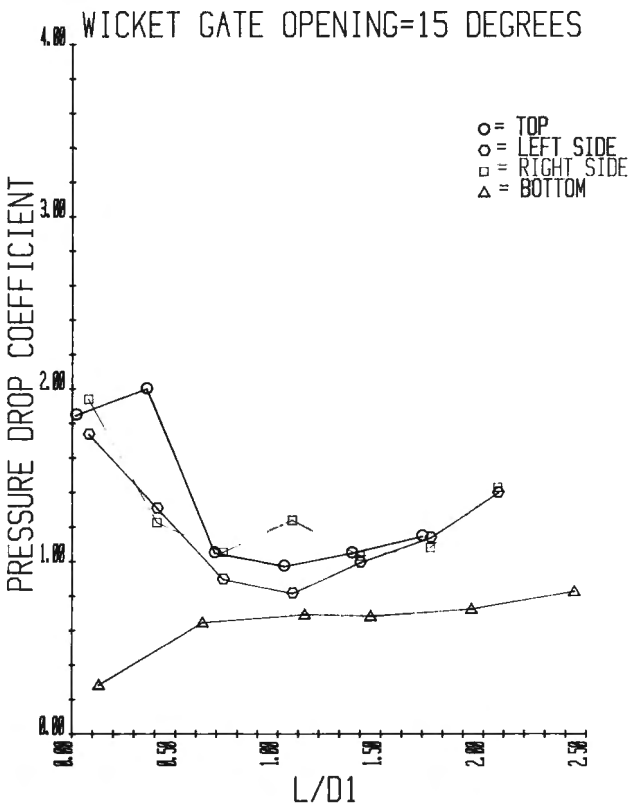

Fig. 11 Pressure drop (C_p) along intake surfaces - intake 2. The uncertainty of the intake pressure drop coefficient is ±0.10.

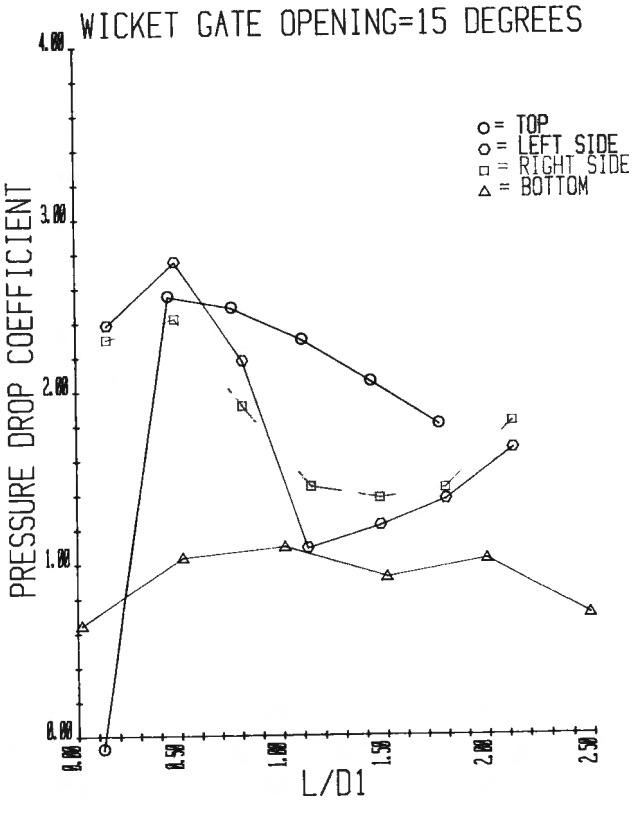

Fig. 12 Pressure drop (C_p) along intake surfaces - intake 3. The uncertainty of the intake pressure drop coefficient is ±0.10.

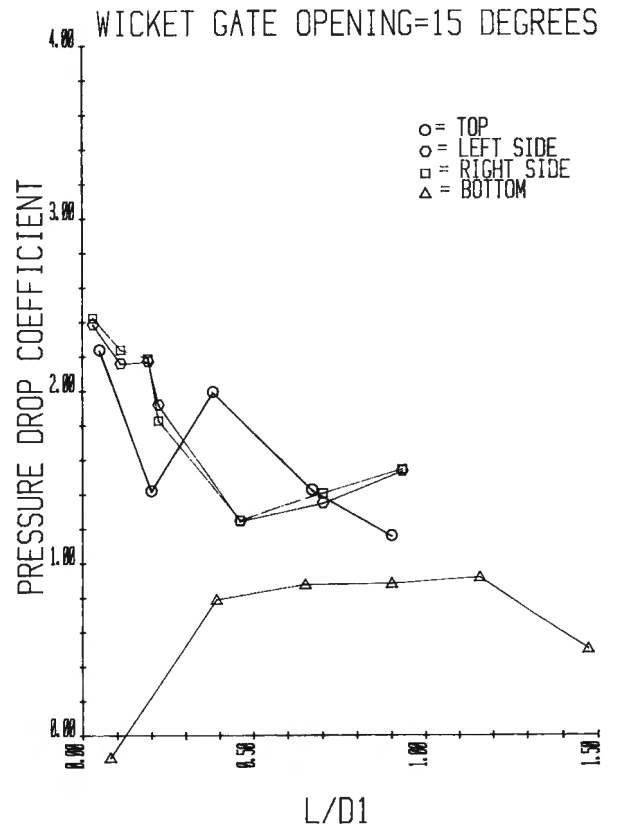

Fig. 13 Pressure drop (C_p) along intake surfaces - intake 4. The uncertainty of the intake pressure drop coefficient is ±0.10.

Pressure drop along the intake surfaces. Pressures were measured along the top, bottom, and sides of each intake (figs 10 through 13). The reference velocity head in C_p for these plots is the average intake velocity head - $(V_I^2/2g)$, where $V_I = V_r/7.026$. For a typical prototype situation the intake velocity head is about 1 percent of the gross head. Intake 3 has the highest local pressure drops. The reference distance (L/D1) is the distance from the front face of the intake to the piezometer (fig 2).

The average pressure at the end of the intake section is an indication of the losses to that point. The average pressure drop coefficients at the end of the intakes were $C_{p1} = 1.216$, $C_{p2} = 1.200$, $C_{p3} = 1.497$, and $C_{p4} = 1.183$, for intakes 1, 2, 3, and 4 (from figs 10 through 13). After subtracting the velocity head from the pressure drops, the energy losses - in terms of intake velocity heads - were 0.216, 0.200, 0.497, and 0.183 for intakes 1 through 4, respectively. This indicates that intake 3 has more than twice as much loss as the others and intake 4 has the lowest losses.

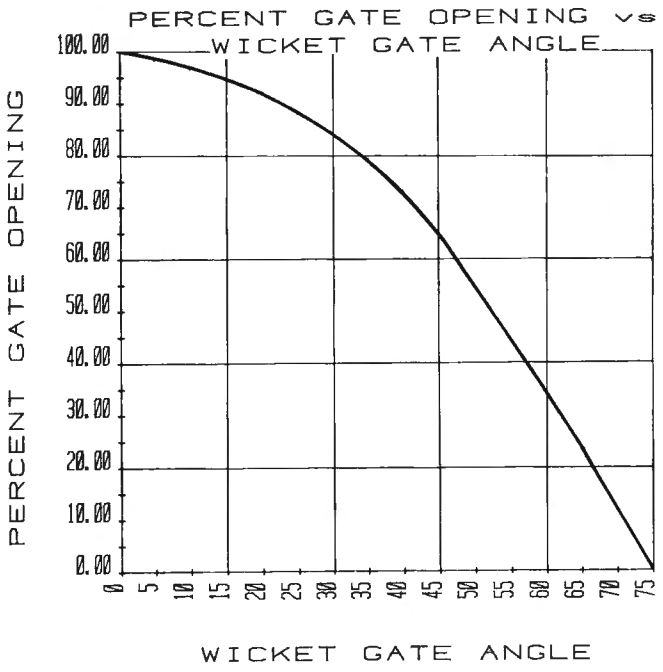

Fig. 14 Percent gate opening vs wicket gate angle.

Percent gate opening in terms of percentage of wicket gate angle is (1 - θ/75) 100, i.e., for θ = 15 deg the gate opening would be 80 percent of the total wicket gate operating range.

It should be noted that the intake velocity head is 50 times less than the runner velocity head. This puts the intake losses in perspective with the overall losses discussed in the previous section.

Wicket Gate Angle vs Percent Gate Opening

Figure 14 is a cross reference for wicket gate angle (θ) vs gate opening, where percent gate opening is defined as (open area)/(open area when the gates are fully open). This figure should be useful in computing losses when the discharge relationship is given in terms of percent gate opening.

CONCLUSIONS

Significant simplifications and size reductions can be made in the intakes of bulb and rim generator turbines without increasing energy losses or adversely affecting flow distribution.

Comparative energy losses and velocity distributions illustrate the advantages of using simplified intake designs.

ACKNOWLEDGMENTS

This research was performed in the Hydraulic Laboratory of the Bureau of Reclamation's Engineering and Research Center under the supervision of T. J. Rhone, Head of the Hydraulic Structures Section, and the general supervision of D. L. King, Chief of the Hydraulics Branch, Division of Research. The work was sponsored by the Department of Energy under agreement EG-77-A-36-1024 with the Bureau of Reclamation.

Dr.-Ing H. T. Falvey and T. J. Rhone provided valuable technical review and comments during the study. Richard Phillips, Robert McGovern, and Cheryl States were instrumental in testing and data reduction.

REFERENCES

1. Pugh, Clifford A., Bureau of Reclamation, "Intakes and Outlets for Low-Head Hydropower," Journal of the Hydraulics Division, ASCE, Vol. 107, No. HY9, Proc. Paper 16494, pp. 1029-1045, September 1981.

2. Strohmer, Franz, Voest-Alpine, "Standardized Runners and Test Results Can Save Small Hydro Costs," World Water, pp. 43-48, November 1981.

3. Kobus, Helmut, German Association for Water Resources and Land Improvement "Hydraulic Modeling," Bulletin 7, pp. 5-6, pp. 288-289, 1978.

4. American Society of Mechanical Engineers, Research Committee on Fluid Meters, "Fluid Meters, Their Theory and Application," pp. 43-85, pp. 142-145, ASME, 1959.

reprinted from

Small Hydro Power Fluid Machinery — 1982
Editors: D.R. Webb, W.G. Whippen, and C.N. Papadakis
(Book No. H00233)

published by

THE AMERICAN SOCIETY OF MECHANICAL ENGINEERS
345 East 47th Street, New York, N.Y. 10017
Printed in U.S.A.